Elastoplastic Analysis by the Integral Equation Method

By

Shoichi KOBAYASHI* and Naoshi NISHIMURA*

(Received March 31, 1980)

Abstract

A method of numerical elastoplastic analysis is presented and several two and three dimensional examples are given.

The elastoplastic velocity field is represented in simple layer and differentiated volume potentials. The boundary condition and flow rule yield a system of singular integral equations which can be solved numerically.

Examples show the high accuracy and efficiency of the present method.

1 Introduction

The integral Equation Method, as a numerical technique to solve linear boundary value problems, is frequently used these days. Nevertheless, only a few works in its application to non-linear problems[1] have been done since 1971, when Swedlow and Cruse[2] showed the method's applicability to elastoplastic boundary value problems. To complicate matters, some of these works are reported to have been based on erroneous formulae.[3),4)] However, we believe this situation by no means indicates that the Integral Equation Method does not have any advantages over conventional methods of elastoplastic analysis. Indeed, the most remarkable aspects of the Integral Equation Method, i.e., the small number on unknowns and the easiness in expressing singularity are both favorable to the end. The former promotes the efficiency of incremental calculation and the latter enables us to give a proper singularity to the elastic-plastic boundary, which may help to improve the accuracy.

In this paper, we formulate a method of numerical elastoplastic analysis based on the simple layer potential method.[5)] The boundary condition and flow rule yield a system of integral equations with a vector valued function on the boundary and a scalar valued function over the plastic region as unknowns. Displacements and stresses are obtained by solving these equations and carrying

* Department of Civil Engineering

out the incremental analysis in an ordinary manner. Several solved two and three dimensional problems are shown as examples. They show the high accuracy and efficiency of the present method.

2 Potential Representation[6]

We assume isotropy in elasticity for simplicity. It can be easily shown that the three dimensional (or plane strain) elastoplastic velocity field $\dot{\boldsymbol{u}}$ is governed by the equations

$$\Delta^*\dot{\boldsymbol{u}}-(\boldsymbol{C}:\dot{\boldsymbol{\varepsilon}}^p)\cdot\nabla=\boldsymbol{0} \qquad \text{in } D^e\cup D^p \tag{1}$$

and

$$\overset{n^{ep}}{\boldsymbol{T}}\dot{\boldsymbol{u}}^- = \overset{n^{ep}}{\boldsymbol{T}}\dot{\boldsymbol{u}}^+-(\boldsymbol{C}:\dot{\boldsymbol{\varepsilon}}^{p+})\cdot\boldsymbol{n}^{ep} \qquad \text{on } \partial D^{ep}, \tag{2}$$

where

$$\Delta^*\boldsymbol{u}=\mu\Delta\boldsymbol{u}+(\lambda+\mu)\nabla\nabla\cdot\boldsymbol{u} \qquad (\Delta^*\text{: Navier operator}), \tag{3}$$

$$\overset{n}{\boldsymbol{T}}\boldsymbol{u}=\lambda\boldsymbol{n}\nabla\cdot\boldsymbol{u}+\mu\left(\frac{\partial\boldsymbol{u}}{\partial\boldsymbol{n}}+(\nabla\boldsymbol{u})\cdot\boldsymbol{n}\right) \qquad (\overset{n}{\boldsymbol{T}}\text{: traction operator}) \tag{4}$$

and

$$\boldsymbol{C}:\boldsymbol{\varepsilon}=\lambda\boldsymbol{1}\,\mathrm{tr}\,\boldsymbol{\varepsilon}+2\mu\boldsymbol{\varepsilon} \qquad (\boldsymbol{C}\text{: elasticity tensor}). \tag{5}$$

D^e, D^p, ∂D^{ep}, $\dot{\boldsymbol{\varepsilon}}^p$, $\boldsymbol{n}^{ep}$, $\cdot$ and: stand for the elastic region, plastic region, elastic-plastic boundary, plastic strain rate (We do not assume $\mathrm{tr}\,\dot{\boldsymbol{\varepsilon}}^p=0$ in this paper.), unit normal vector on ∂D^{ep} directed toward D^e, $\cdot i\cdot i$ and $\cdot ij\cdot ij$ type inner products, respectively. A superposed $+(-)$ denotes a limiting value on ∂D^{ep} from D^p (D^e). Note $\dot{\boldsymbol{\varepsilon}}^{p+}\neq\boldsymbol{0}$ in general.

Motivated by eqs. (1) and (2), we put

$$\dot{\boldsymbol{u}}=\int_{\partial D}\boldsymbol{\Gamma}\cdot\dot{\boldsymbol{\varphi}}dS+\int_{D^p}\boldsymbol{\Gamma}\cdot\dot{\boldsymbol{\psi}}dV+\int_{\partial D^{ep}}\boldsymbol{\Gamma}\cdot\dot{\boldsymbol{\varphi}}^{ep}dS, \tag{6}$$

where $\boldsymbol{\Gamma}$ is the fundamental solution of elasticity, or Kelvin's point load solution. Substituting eq. (6) into eqs. (1) and (2), we have

$$\dot{\boldsymbol{\psi}}+(\boldsymbol{C}:\dot{\boldsymbol{\varepsilon}}^p)\cdot\nabla=\boldsymbol{0} \tag{7}$$

and

$$\dot{\boldsymbol{\varphi}}^{ep}-(\boldsymbol{C}:\dot{\boldsymbol{\varepsilon}}^p)\cdot\boldsymbol{n}^{ep}=\boldsymbol{0}. \tag{8}$$

Using Gauss' theorem, we have

$$\dot{\boldsymbol{u}}=\int_{\partial D}\boldsymbol{\Gamma}\cdot\dot{\boldsymbol{\phi}}dS+\int_{D^p}\boldsymbol{\Gamma}\overleftarrow{\nabla}:(\boldsymbol{C}:\dot{\boldsymbol{\varepsilon}}^p)dV, \tag{9}*$$

* For numerical calculation, not $\Gamma_{ij,k}$ but $\Gamma_{i(j,k)}$ is recommended.

where

$$\dot{\boldsymbol{\phi}} = \dot{\boldsymbol{\varphi}} \mp (\boldsymbol{C}: \dot{\boldsymbol{\varepsilon}}^p) \cdot \boldsymbol{n} \tag{10}$$

with the upper (lower) sign taken for interior (exterior) problems. (This convention will be used in what follows.)

It might be possible to use eq. (9) and the flow rule for numerical elastoplastic analysis, but a more effective approach is found by examining the form of the flow rule. We assume that a yield function $f(\boldsymbol{\tau}, \boldsymbol{\psi})$ describes admissible states by the condition

$$f(\boldsymbol{\tau}, \boldsymbol{\psi}) \leqslant 0\,, \tag{11}$$

where $\boldsymbol{\tau}$ and $\boldsymbol{\psi}$ stand for stress and a set of internal parameters, respectively, and that the time variation of $\boldsymbol{\psi}$ is governed by an evolutional equation

$$\dot{\boldsymbol{\psi}} = \boldsymbol{\Theta}(\boldsymbol{\tau}, \boldsymbol{\psi}): \dot{\boldsymbol{\varepsilon}}^p\,. \tag{12}$$

Under these assumptions, the (associated) plastic strain rate takes the following form:

$$\dot{\boldsymbol{\varepsilon}}^p = \frac{\partial f}{\partial \boldsymbol{\tau}} \boldsymbol{D}: \dot{\boldsymbol{\varepsilon}}\,, \tag{13}$$

where $\dot{\boldsymbol{\varepsilon}}$ is strain rate,

$$\boldsymbol{D} = \frac{\dfrac{\partial f}{\partial \boldsymbol{\tau}}: \boldsymbol{C}}{\dfrac{\partial f}{\partial \boldsymbol{\tau}}: \boldsymbol{C}: \dfrac{\partial f}{\partial \boldsymbol{\tau}} - \dfrac{\partial f}{\partial \boldsymbol{\psi}} * \boldsymbol{\Theta}: \dfrac{\partial f}{\partial \boldsymbol{\tau}}} \tag{14}$$

and $*$ signifies a certain product. Using eq. (13), we have

$$\dot{\boldsymbol{u}} = \int_{\partial D} \boldsymbol{\Gamma} \cdot \dot{\boldsymbol{\phi}} dS + \int_{D^p} \boldsymbol{\Gamma} \nabla: \left(\boldsymbol{C}: \frac{\partial f}{\partial \boldsymbol{\tau}} \right) \dot{\Psi} dV \tag{15}$$

and

$$\dot{\Psi} = \boldsymbol{D}: \dot{\boldsymbol{\varepsilon}}\,. \tag{16}$$

The boundary condition and flow rule (eq. (16)) yield a system of integral equations with $\dot{\boldsymbol{\phi}}$ and $\dot{\Psi}$ as unknown functions, which can be solved numerically. Note $\dot{\boldsymbol{\phi}}$ is a vector function defined on ∂D, and $\dot{\Psi}$ is a scalar function defined over D^p.

Using eq. (9), we obtain integral equations corresponding to the boundary condition and flow rule. To this end, we calculate $\nabla \boldsymbol{u}$ in D^p and its limiting value on ∂D. For the three dimensional case, we have

$$\nabla \boldsymbol{u} = \boldsymbol{V}: (\boldsymbol{C}: \dot{\boldsymbol{\varepsilon}}^p) + \int_{\partial D} \nabla \boldsymbol{\Gamma} \cdot \dot{\boldsymbol{\phi}} dS + \int_{D^p} \nabla \boldsymbol{\Gamma} \nabla: (\boldsymbol{C}: \dot{\boldsymbol{\varepsilon}}^p) dV \tag{17}$$

in D^p, where

$$\boldsymbol{V}:\boldsymbol{\varepsilon}=\frac{1}{15\mu}\left(\frac{3\lambda+8\mu}{\lambda+2\mu}\boldsymbol{\varepsilon}-\frac{\lambda+\mu}{\lambda+2\mu}\mathbf{1}\ \mathrm{tr}\,\boldsymbol{\varepsilon}\right) \tag{18}$$

and $\int_{D^p}$ denotes the ordinary principal value integral, which is clearly convergent. The limiting value on ∂D may be easily calculated as

$$\nabla\dot{\boldsymbol{u}}=\pm\overset{*}{\boldsymbol{S}}\cdot(\dot{\boldsymbol{\phi}}\pm(\boldsymbol{C}:\dot{\boldsymbol{\varepsilon}}^p)\cdot\boldsymbol{n})+\frac{1}{2}\boldsymbol{V}:(\boldsymbol{C}:\dot{\boldsymbol{\varepsilon}}^p)+$$
$$+\int_{\partial D}\nabla\boldsymbol{\Gamma}\cdot\dot{\boldsymbol{\phi}}dS+\int_{D^p}\nabla\boldsymbol{\Gamma}\nabla:(\boldsymbol{C}:\dot{\boldsymbol{\varepsilon}}^p)dV \tag{19}$$

where

$$\overset{*}{\boldsymbol{S}}\cdot\boldsymbol{\phi}=\frac{1}{2\mu}\left(\boldsymbol{n}\otimes\boldsymbol{\phi}-\frac{\lambda+\mu}{\lambda+2\mu}(\boldsymbol{n}\cdot\boldsymbol{\phi})\boldsymbol{n}\otimes\boldsymbol{n}\right) \tag{20}$$

and $\int_{D^p}$ indicates the principal value integral defined as

$$\lim_{\varepsilon\downarrow 0}\int_{D\setminus B_\varepsilon}\cdot\,dV,\quad B_\varepsilon=\{\boldsymbol{x}\,|\,|\boldsymbol{x}-\boldsymbol{x}_0|<\varepsilon,\ \boldsymbol{x}\in D,\ \boldsymbol{x}_0\in\partial D\}$$

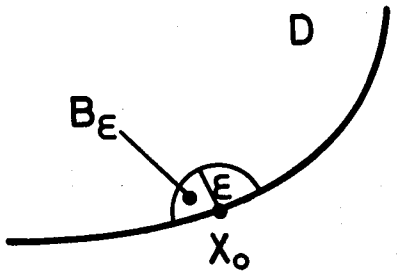

Fig. 1. Domains for the definition of principal value integral.

which can be easily shown to converge in this case. Using eqs. (14)-(17) and (19), we may obtain a system of integral equations with $\dot{\boldsymbol{\phi}}$ and $\dot{\Psi}$ as unknown functions.

It is by no means easy to see the solvability of the obtained integral equations. For traction boundary value problems, however, we can easily establish the existence of $\dot{\boldsymbol{\phi}}$ for the given sufficiently smooth boundary traction $\dot{\boldsymbol{t}}$ and $\dot{\boldsymbol{\varepsilon}}^p$, provided ∂D is sufficiently smooth and, for the interior problem, $\int_{\partial D}\dot{\boldsymbol{t}}dS=\mathbf{0}$ and $\int_{\partial D}\boldsymbol{x}\times\dot{\boldsymbol{t}}dS=\mathbf{0}$. Thus, the assumption made in eq. (6) is justified.

Before closing this section we discuss briefly some extensions of the present formulation.

1) In order to express a far-off field, we may add $\dot{\boldsymbol{u}}_0$, which satisfies $\Delta^*\dot{\boldsymbol{u}}_0=\boldsymbol{0}$, to the right hand side of eq. (9).

2) We have considered three dimensional or plane strain cases so far. However, the whole analyses leading to eqs. (15) and (16) apply to plane stress case, with λ replaced by $2\mu\lambda/(\lambda+2\mu)$ and tr in eq. (15) taken as the two dimensional one.

3) We assumed the regularity of the yield surface, or the existence of one yield function. The cases with several yield functions may be treated similarly, resulting in an analogue of eq. (15) with as many unknown functions $\dot{\Psi}_i$ in D^p as the yield functions which are calculated as zero.

4) Crack problems may be solved by adding a double layer potential over the crack surface to eq. (15).

3 Numerical Analysis

The method of analysis employed here is rather conventional, i.e., the discretization of unknown functions by appropriate shape functions, the numerical solution of the resulting system of algebraic equations and incremental evaluation of field quantities. In this section, we discuss these steps briefly.

1) Discretization

We use the simplest method of discretization, i.e., the modelling of ∂D and D^p by an assemblage of plane and polyhedral segments, and the interpolation of the unknown quantities by the characteristic functions of these segments. Then, all the integrals appearing in the discretized counterpart of eq. (9) can be calculated analytically. By direct differentiation and some limit calculations, if necessary, we can construct the discretized boundary condition and flow rule without reference to eqs. (17) and (19). Piecewise constant approximation is considered to be the simplest reasonable one for our potential representation, though unreasonable for the Swedlow-Cruse type representation because the boundary stresses of the double layer potential depend on the derivatives of its density explicitly.

The modelling of D^p requires some intuition. The region where yielding is likely to occur must be subdivided into mesh in advance.

2) Numerical solution of the integral equations

We take $\dot{\boldsymbol{\phi}}$ and $\dot{\Psi}$ as unknown functions. Collocation is used to discretize the boundary condition and flow rule. These equations are solved simultaneously using a direct method (Crout method) so that iterative computation is not necessary for each incremental step. Although some parts of the coefficient matrix

alter for each step, the size is small because $\dot{\Psi}$ is a scalar function.

3) Incremental analysis

Ordinary incremental analysis is employed and no corrective iteration is carried out. The magnitude of each increment is determined so as to make one element yield in one step. Note that the sign of $\dot{\Psi}$ determines the state of the corresponding element, i.e., $\dot{\Psi}>0$ for loading, $\dot{\Psi}=0$ for neutral and $\dot{\Psi}<0$ for unloading.

4 Examples

Several two and three dimensional boundary value problems are solved by using the method described in §3.

1) Extension of circular hole[7]

It is well-known that the above mentioned problem admits analytical solutions for statically determinate stresses under some assumptions, i.e., plane strain, Tresca's yield condition and no work hardening. As was noted by R. Hill, these solutions also approximate stress states in von Mises material under the same conditions, with a slight modification. Assuming perfectly elastic-plastic von Mises material, we computed several stresses and compared the results with analytical solutions. The material properties were set as follows:

E (Young's modulus) $= 2.1\times10^6$ kg/cm^2 (206 GPa), ν (Poisson's ratio) $= 0.3$,
σ_y (yield stress) $= 2500$ kg/cm^2 (245 MPa) .

$\tau_{\theta\theta}$ and τ_{rr} for p (internal pressure) $=0.6$, 0.66 and 0.8 σ_y, calculated at several points using the model shown in Fig. 2, are plotted in Figs. 3 and 4. They agree well with the analytical solutions shown by the solid line in spite of the ra-

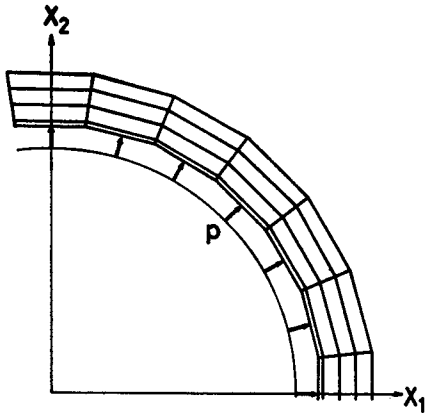

Fig. 2. Model of circular hole.

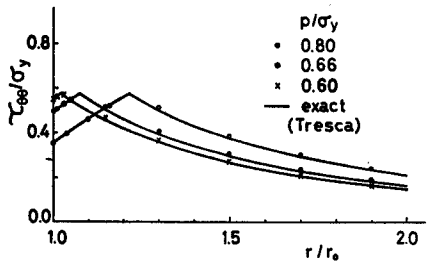

Fig. 3. Hoop stress around a circular hole subject to internal pressure.

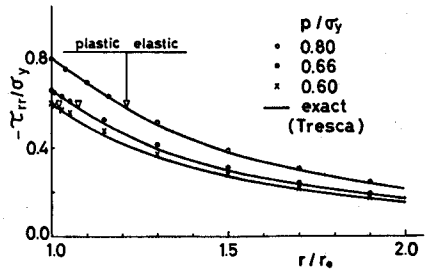

Fig. 4. τ_{rr} around a circular hole subject to internal pressure.

ther coarse mesh used.

2) Circular hole subject to biaxial tension[8)]

Using the complex potential technique, L.A. Galin calculated stresses around a circular hole subject to biaxial tension under several assumptions, i.e., plane strain, incompressibility (Tresca or von Mises yield condition) and no work hardening. We solved the same problem under the following conditions:

$$E = 2.1 \times 10^6\ \mathrm{kg/cm^2}\ (206\ \mathrm{GPa}),\ \nu = 0.45,\ \sigma_y = 2500\ \mathrm{kg/cm^2}\ (245\ \mathrm{MPa}),$$
$$\tau_{11}^{\infty} = 1875\ \mathrm{kg/cm^2}\ (184\ \mathrm{MPa},\ 0.75\sigma_y),\ \tau_{22}^{\infty} = 2125\ \mathrm{kg/cm^2}\ (208\ \mathrm{MPa},\ 0.85\sigma_y)\ .$$

The choice for Poisson's ratio may make the result a close approximation of the incompressible solution though an exact incompressible analysis might be possible within our framework after some limit calculations, which the authors do not think worth while.

The calculated plastic region is shown in Fig. 5, which agrees quite well with the exact one depicted by a solid line. (The subdivision used is also shown in Fig. 5.) τ_{22} along x_1 axis and τ_{11} along x_2 axis are plotted in Figs. 6 and 7, which

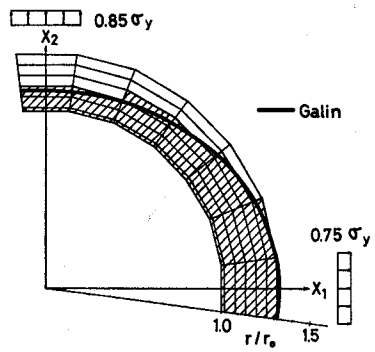

Fig. 5. Plastic region around a circular hole subject to biaxial tension.

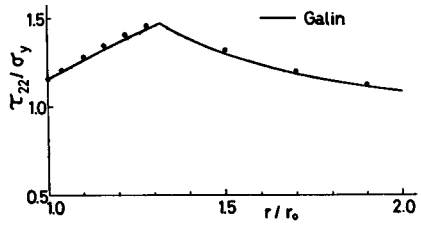

Fig. 6. τ_{22} along x_1 axis; circular hole subject to biaxial tension.

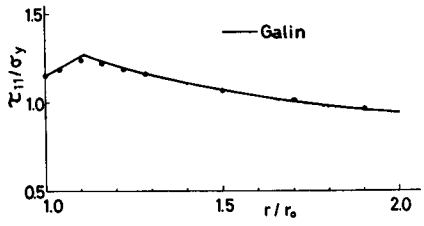

Fig. 7. τ_{11} allong x_2 axis; circular hole subject to biaxial tension.

are also in excellent agreement with Galin's results.

CPU time was about 16 sec., using M190 at the Kyoto University Data Processing Center.

3) Three dimensional tunnel analysis

A three dimensional elastoplastic analysis was carried out in order to estimate the size of the plastic region around a tunnel under excavation. This kind of analysis is important for the mechanical interpretation of the so called NATM (New Austrian Tunnelling Method).

For simplicity, we assumed that the mechanical behaviour of rock can be modelled by elastic-plastic material with the Drucker-Prager yield condition and associated flow rule. The material properties were put as follows:

$E = 7000\ \mathrm{kg/cm^2}$ (686 MPa), c (cohesion) $= 20\ \mathrm{kg/cm^2}$ (1.96 MPa),
$\nu = 0.4$, ϕ (friction angle) $= 30°$.

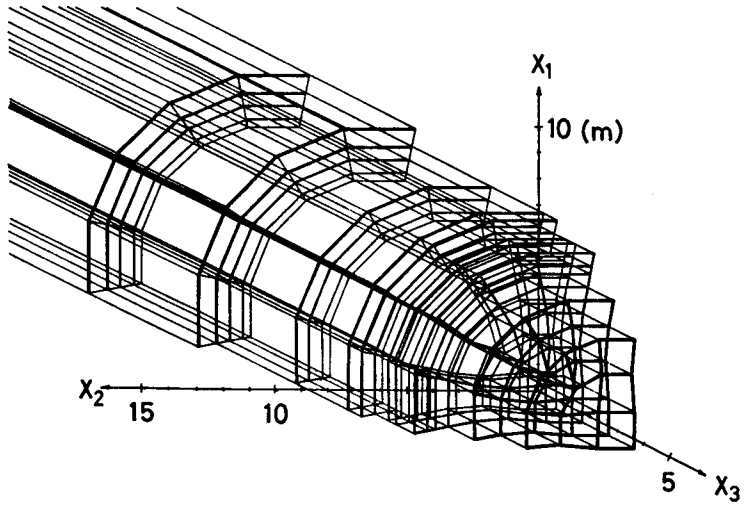

Fig. 8. Model of tunnel under excavation.

Also, a slight isotropic hardening was assumed to c. The initial stress state was set as $\tau_{11}^0=-60$ kg/cm^2 (5.88 MPa), $\tau_{22}^0=\tau_{33}^0=-80$ kg/cm^2 (7.84 MPa), in the cartesian coordinate system shown in Fig. 8. The tunnel cross section is assumed to be a circle having a diameter of 10 m.

Fig. 9 shows the plastic region obtained by using the mesh shown in Fig. 8.

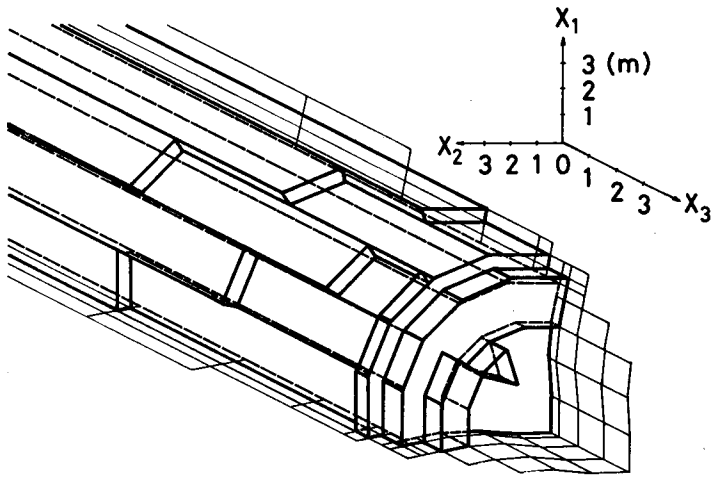

Fig. 9. Plastic region; three dimensional tunnel analysis.

The plastic region grows vertically (in the x_1 direction) at the side of the tunnel, but no such trend is seen near the face. Also, we see that the thickness of the plastic region on the side diminishes as the face is approached. This effect may be considered to be of fundamental importance in understanding the mechanical

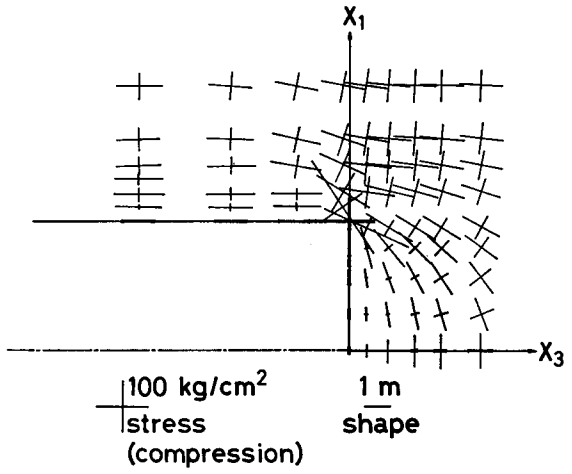

Fig. 10. Principal stress in x_1-x_3 plane; three dimensional tunnel analysis.

aspects of tunnel excavetion. Figs. 10 and 11 show the in-plane princiapl stress and τ_{22} in x_1-x_3 plane, respectively. The displacements on the boundary are given in Fig. 12. The vertical component in the x_1-x_3 plane is amplified, com-

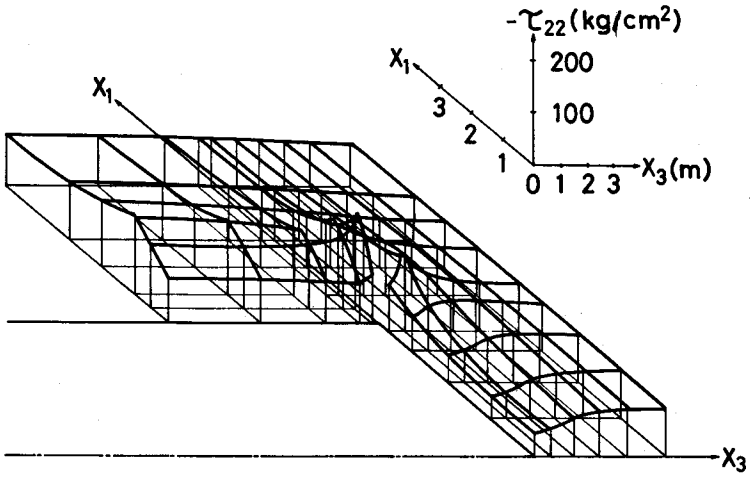

Fig. 11. τ_{22} in x_1-x_3 plane; three dimensional tunnel analysis.

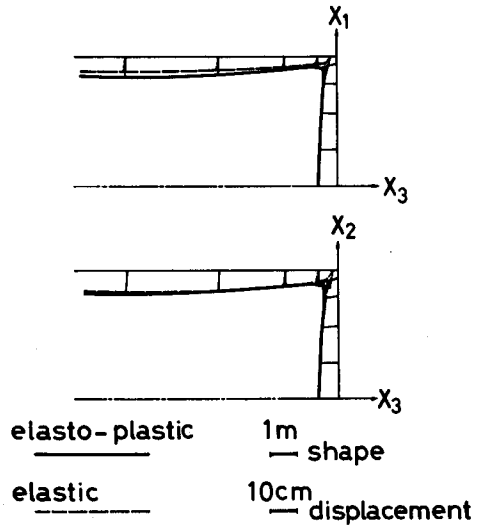

Fig. 12. Displacement on the boundary; three dimensional tunnel analysis.

pared with the elastic displacement expressed by a broken line, showing the effect of the plastic intrusion.

The analysis in 75 steps was carried out in 10 minutes of CPU time using M190 at the Kyoto University Data Processing Center.

5 Concluding Remarks

1) P.K. Banerjee et al.[9] proposed to convert the volume integral in eq. (9) into the volume potential over D^p. However, this process is not reasonable because eq. (9) is equivalent to eq. (6) and $\dot{\boldsymbol{\varepsilon}}^{p+} \neq \boldsymbol{0}$ on ∂D^{ep} in general. Such a conversion may be acceptable if eq. (6) is integrated with respect to time.

2) In effect, eqs. (17) and (19) were not used in our numerical analysis. However, the importance of these equations is twofold. Firstly, they show that the stresses in D^p and on ∂D do not depend explicitly on the derivatives of potential densities, so that the piecewise constant approximation may be considered reasonable. Secondly, they become necessary if a higher order intepolation is employed, where numerical integration is indispensable.

An analogue of eq. (17) was also noted by Bui[4].

3) The most time consuming part in the algorithm of the Integral Equation Method is the evaluation of integrals. Therefore, the simple layer potential approach shown in this paper may be more practical than the Swedlow-Cruse type formulation, considering the number of integrations needed.

4) We took $\dot{\boldsymbol{\phi}}$ and $\dot{\Psi}$ as unknown functions. As $\dot{\Psi}$ is a scalar function, the resulting linear algebraic equation is small in size, especially in a the three dimensional case. Thus, the present method may be applied effectively to almost any boundary value problems.

References

1) Mendelson, A.: Boundary-Integral Methods in Elasticity and Plasticity, NASA, TN D-7418, 1973.
Mendelson, A. and L.U. Albers: Application of Boundary Integral Equations to Elastoplastic Problems, Boundary-Integral Equation Method: Computational Applications in Applied Mechanics (Ed. by T.A. Cruse and F.J. Rizzo), Proc. ASME, AMD-Vol. 11, 1975.
2) Swedlow, J.L. and T.A. Cruse: Int. J. Solids Struct., Vol. 7, pp 1673–1683, 1971.
3) Mukherjee, S.: Int. J. Solids Struct., Vol. 13, pp 331–335, 1977.
4) Bui, H.D.: Int. J. Solids Struct., Vol. 14, pp 935–939, 1978.
5) Kupradze, V.D.: Potential Methods in the Theory of Elasticity (Tr. by H. Goftreund), Israel Program for Scientific Translations, Jerusalem, 1965.
6) Kobayashi, S. and N. Nishimura: to appear in Proc. JSCE (in Japanese).
7) Hill, R.: The Mathematical Theory of Plasticity, Oxford, 1950.
8) Savin, G.N.: Stress Concentration around Holes (Tr. by E. Gros), Pergamon, 1961.
9) Banerjee, P.K. and G.G. Mastoe: The Boundary Element Method for Two-Dimensional Problems of Elastoplasticity, Recent Advances in Boundary Element Methods (Ed. by C.A. Brebbia), Pentech Press, 1978.